Preparation and Characterization of Visible-Light-Driven Carbon–Sulfur-Codoped TiO 2 Photocatalysts

ARTICLE *in* INDUSTRIAL & ENGINEERING CHEMISTRY RESEARCH · JULY 2006

Impact Factor: 2.59 · DOI: 10.1021/ie060350f

MATERIALS AND INTERFACES

Preparation and Characterization of Visible-Light-Driven Carbon−Sulfur-Codoped TiO_2 Photocatalysts

Hongqi Sun, Yuan Bai, Youping Cheng, Wanqin Jin,* and Nanping Xu

Membrane Science and Technology Research Center, Nanjing University of Technology, 5 Xinmofan Road, Nanjing 210009, P. R. China

A novel photocatalyst, carbon−sulfur-codoped TiO_2 (TCS) was synthesized by the hydrolysis of tetrabutyl titanate in a mixed aqueous solution containing thiourea and urea. The codoped TiO_2 was also prepared directly by calcining amorphous or anatase TiO_2 with a mixture of thiourea and urea. The as-prepared powders were characterized by X-ray diffraction (XRD), UV−visible reflectance spectroscopy, X-ray photoelectron spectroscopy (XPS), Fourier transform infrared spectroscopy, and thermal analysis−thermogravimetry (TG-DSC). The photocatalytic activity was evaluated by the photodegradation of 4-chlorophenol under both UV and visible irradiation. By investigating the crystal structures, optical properties, and photocatalytic activities of various samples, we found that the wet chemistry process and the crystal transition process from amorphous to anatase seemed to be critical to the doping process.

1. Introduction

Titanium dioxide (TiO_2) has been studied as a promising photocatalyst for several decades because of the application of solar energy conversion, air purification, and organic contaminant photodegradation.[1] However, TiO_2 can activate only in the low-UV region (<400 nm), about 4% of the incoming solar energy, because of its large band gap of about 3.2 eV. To effectively utilize visible light, which represents about 42% of the energy of the solar spectrum, much effort has been directed toward the development of nonmetal-ion-doped TiO_2. In 1986, Sato first prepared nitrogen-doped TiO_2 as a visible photocatalyst that had a visible response ability.[2] Asahi et al. developed nitrogen-doped TiO_2 that could lower the band gap of TiO_2 and shift the optical response to the visible region.[3] Thereafter, nitrogen-doped TiO_2 attracted much attention from various research groups.[4−7] In addition, some other kinds of nonmetal ions have been found to be capable of making doped TiO_2 respond to visible radiation, such as carbon,[8−11] sulfur,[12,13] fluorine,[14] iodine,[15] and phosphorus.[16] The doped ions depend, to some extent, on ion donors. Thus, the selection of ion donors is important in the preparation of nonmetal-ion-doped photocatalysts. Among reported ion donors, thiourea and urea have often been used because they are potential donors of sulfur, nitrogen, and carbon. For instance, thiourea has been used as a sulfur donor[9] and as a nitrogen donor,[4,17] urea has been used as a nitrogen donor,[5,17] and both thiourea and urea were used together as a carbon donor.[10] However, few studies have focused on producing codoped TiO_2 using thiourea or urea as the ion donor.[18]

In this study, therefore, both thiourea and urea were applied as ion donors to prepare carbon−sulfur-codoped TiO_2 photocatalysts using tetrabutyl titanate as the precursor. The prepared codoped TiO_2 catalysts exhibited a visible response attributable to the doping of carbon and sulfur.

2. Experimental Section

2.1. Sample Preparation. To synthesize carbon−sulfur-codoped TiO_2 particles, 11.65 g (0.3 mol) of thiourea (99.0%, SCR) and 9.10 g (0.3 mol) of urea (99.0%, SCR) were dissolved in 150 mL of pure water and magnetically stirred for 30 min. At that point, 26 mL (0.075 mol) of tetrabutyl titanate (98.0%, SCR) as the precursor was slowly added to the solution while it was surrounded by an ice bath. Then, the mixed solution was stirred for 12 h and aged for 24 h, and the water was removed at 80 °C in air. The precipitate was finally calcined at 500, 550, or 600 °C for 3 h in a muffle oven at a heating rate of 5 °C·min^{-1}. The obtained catalysts are denoted as TCS1, TCS2, and TCS3, respectively. To compare the effects of the preparation methods on the activity of the photocatalyst, codoped TiO_2 photocatalysts were also prepared directly by calcining amorphous TiO_2 or anatase TiO_2 with a mixture of thiourea and urea at 600 °C; these samples are denoted as TCS4 and TCS5, respectively. The powders before calcination are denoted as TCS1/p, TCS2/p, TCS3/p, TCS4/p, and TCS5/p, respectively. Pure TiO_2 was prepared by direct hydrolysis of tetrabutyl titanate in water surrounded by an ice bath.

2.2. Characterization. The crystallization behavior was monitored using a Netzsch STA409 TG-DSC instrument, in the temperature range from room temperature to 800 °C. Fourier transform infrared spectroscopy was preformed on a Thermo Nicolet AVATAR-360 spectrometer in the range of 4000−400 cm^{-1} by the KBr pellet method. X-ray diffraction (XRD) patterns were obtained on a Bruker D8-Advance X-ray diffractometer using Cu Kα radiation (λ = 1.5405 Å) to determine the crystalline phase and the lattice parameters. The accelerating voltage and the applied current were 40 kV and 30 mA, respectively. The XRD patterns of the (101) plane were investigated in the scanning range 2θ 24.5−26.0° at a scanning

* To whom correspondence should be addressed. Tel.: +86-25-83587211. Fax: +86-25-8358-7211. E-mail: wqjin@njut.edu.cn.

10.1021/ie060350f CCC: $33.50
Published on Web 06/15/2006

rate of 0.01° s^{-1}. The average crystalline sizes were calculated by the Scherrer formula according to the literature.[6] The phase contents of the samples were calculated from the integrated intensities of the anatase (101), rutile (110), and brookite (121) peaks.[15] The lattice parameters were obtained from the full-profile structure refinement of the XRD data using powder indexing. UV−vis reflectance spectra were measured with a Shimadzu UV-2401TC UV−vis spectrophotometer, using $BaSO_4$ as the background. The spectra were used to evaluate the optical properties of the samples.[7] The states of the charges were investigated by X-ray photoelectron spectroscopy (XPS) using an ESCALab MK2 instrument with a Mg X-ray source and employing Ar^+ sputtering to remove the surface layer of the sample.

2.3. Photodegradation of 4-Chlorophenol. The photocatalytic activity of the carbon−sulfur-codoped TiO_2 photocatalyst was evaluated by measuring the degradation efficiency of 4-chlorophenol (1.5×10^{-4} mol L^{-1}) under visible irradiation. Photodegradation experiments were carried out with 100-mg samples of powder suspended in 100 mL of a 4-chlorophenol (4-CP) solution in a 250-mL reactor. A recycling water jacket was used to keep the reactor temperature constant at 30 ± 1 °C. A 250-W Xe lamp (L25, Haolang Opticlight; $\lambda_{max} = 470$ nm) was used as the visible light source, which irradiated outside (at a distance of 25 cm from the solution surface) through a 400-nm-cutoff filter (L40, Libang) onto the reactor. The light intensity near the solution surface was about 30 mW cm^{-2}. Experiments on the photocatalytic degradation of 4-CP under UV irradiation were carried out by the same method without the cutoff filter and with a 250-W high-pressure mercury lamp as the UV source. The concentration of 4-CP was determined by measuring the decrease of the absorbance at 225 nm.[8]

3. Results and Discussion

3.1. Thermal Analysis. Figure 1A displays DSC curves of three samples (TCS3/p, TCS4/p, and TCS5/p) before calcination. The first endothermic peak at around 100 °C is due to the desorption of water and alcohol, and the other endothermic peak at about 220 °C arises from the decomposition of thiourea and urea. The first strong exothermic peak at about 265 °C can be attributed to the combustion of organic substances dispersed at the particle level, the second exothermic peak at about 428 °C is due to the combustion of organic substances dispersed at the molecule level, and the third exothermic peak at about 460 °C is caused by the formation of the anatase phase. The temperature of the third exothermic peak was higher than the average data by about 60 °C, which can be attributed to the effects of the decomposition and combustion of thiourea and urea.

Figure 1B shows TG curves of three samples (TCS3/p, TCS4/p, and TCS5/p) before calcination. Below 100 °C, the mass loss of TCS3/p (1.5%) is greater than those of TCS4/p (0.3%) and TCS5/p (0.4%) because of the water and alcohol in TCS3/p derived from the wet chemistry process. The mass loss from 100 to 250 °C can be attributed to the decomposition of thiourea and urea. In this region, most of the organic components in TCS5/p (65.8%) decomposed, and the mass loss was much larger than those of TCS3/p (51.8%) and TCS4/p (57.7%). The mass loss from 250 to 310 °C might be due to the combustion and carbonization of the organic substances in the powders. From 370 to 500 °C, the rate of mass loss of TCS3/p (from 51.8% to 85.2%) was larger than those of the other two samples (from 57.7% to 86.5% for TCS4/p and from 65.8% to 87.2% for TCS5/p). The TG differences among the three samples are thought to be due to the dispersion size, as discussed in the next section.

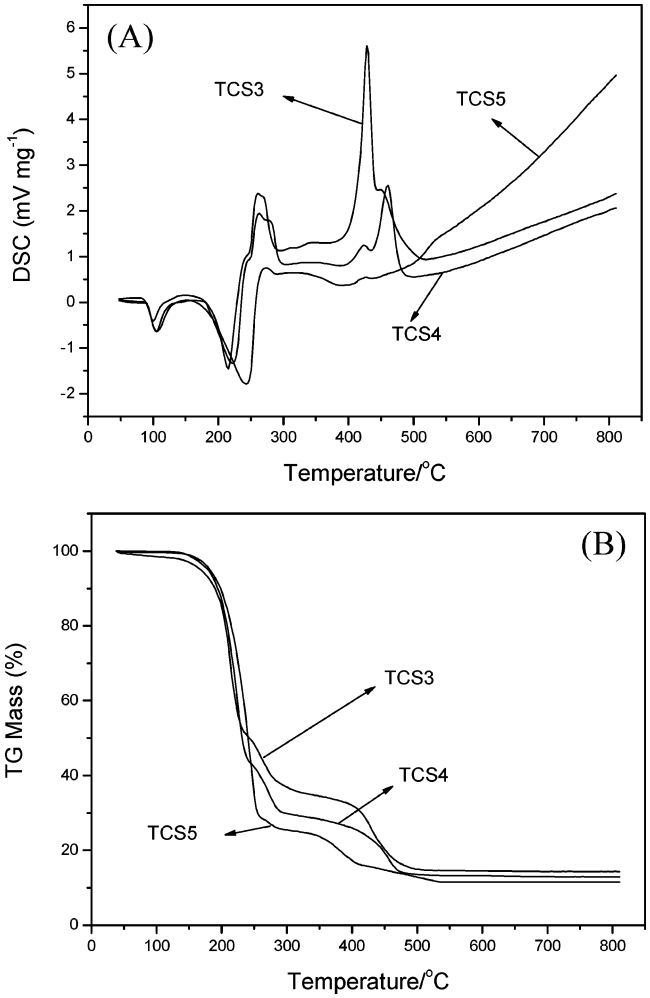

Figure 1. (A) DSC and (B) TG curves of TCS3, TCS4, and TCS5 before calcination.

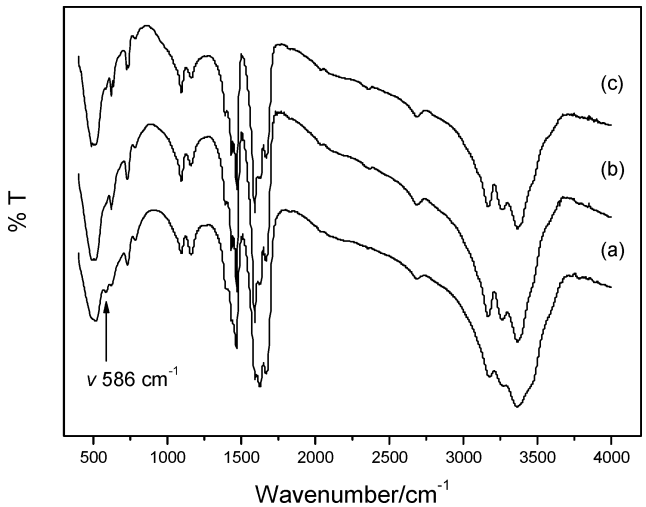

Figure 2. FT-IR spectra of various samples before calcination: (a) TCS3/p, (b) TCS4/p, (c) TCS5/p.

3.2. FT-IR Spectrum Analysis. Figure 2 displays the FT-IR spectra of the powders before calcination. The FT-IR spectra of three samples, TCS3/p, TCS4/p, and TCS5/p remain almost unchanged. Most of the bonds are indexed to C═O (1667 cm^{-1}), C−H (1446 cm^{-1}), $-NH_2$ (3258, 3360 cm^{-1}), C−N (1386 cm^{-1}), C═S (1165 cm^{-1}), Ti−O (520 cm^{-1}), and −OH (3300, 620 cm^{-1}) radicals of the samples.[18] The bands of TCS3/p have no difference from the others, except for an additional υ

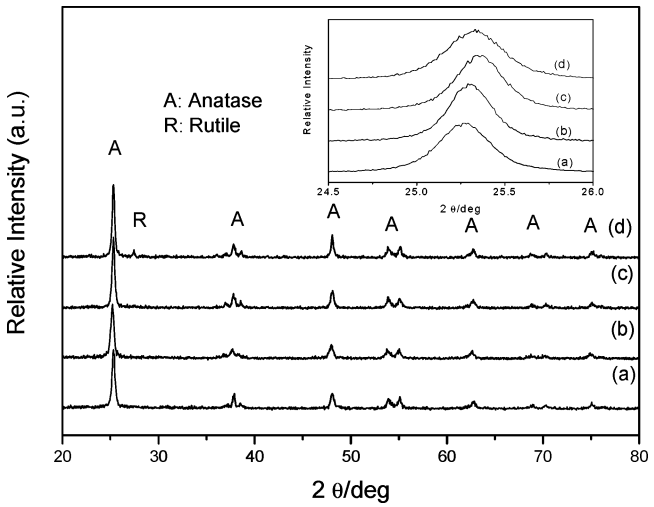

Figure 3. XRD patterns of pure TiO_2 and codoped TiO_2 prepared by different methods: (a) pure TiO_2, (b) TCS3, (c) TCS4, (d) TCS5. Inset: XRD patterns of the (101) plane.

Ti−S absorption band at about 586 cm^{-1}. [19] This peak is thought to arise as a result of the wet chemistry process.

From the FT-IR spectra, we found that no additional new radicals participate in the wet chemistry process, except a small amount of Ti−S. In the powders of TCS3/p, some of the thiourea and urea mixed with TiO_2 at the molecule level, whereas in the samples of TCS4/ p and TCS5/p, most of the thiourea and urea mixed with anatase or brookite TiO_2 at the particle level. It is known that the activity of composite materials depends on both the blending and the much lower-scaled structure of the component materials.[20] The uniformity or nonuniformity of mixtures must be considered at various length scales.[21] Thus, the differences in the structures and optical properties of TCS3 and TCS4 might be attributable to a variation in the spatial distribution of the components of these powders before calcination. These differences between TCS4 and TCS5 might be caused by different crystal phases.

3.3. Crystal Structure. Figure 3 shows XRD patterns of pure TiO_2 and C−S-codoped TiO_2. Pure TiO_2 mainly consists of the anatase phase with little brookite content. TCS3 and TCS4 are pure anatase phase. TCS5 is predominantly anatase phase with a small amount of rutile phase (corresponding to the peak at $2\theta = 27.5°$) due to further calcination of the mixture of anatase TiO_2 and ion donors. The XRD patterns of the (101) plane of pure TiO_2, TCS3, TCS4, and TCS5 are shown in the inset of Figure 3. Compared to pure TiO_2, the peak of the (101) surface of TCS5 shifts slightly to higher values of 2θ. The shifts of TCS3 and TCS4, which are larger than that of TCS5, are almost equal. The shift of the (101) peak shows the lattice distortion of the codoped photocatalysts. This conclusion is supported by the results of the calculation of the lattice parameters of various samples. Table 1 lists the calculated values of the crystalline particle sizes, crystal phase contents, and lattice parameters. Pure TiO_2 and TCS2 were calcined at 550 °C. The crystalline particle size of pure TiO_2 is larger than that of TCS2, and its anatase phase content is greater than that of TCS2. The organic substances and the dopants hinder the expansion of the crystalline particle size and suppress the phase transition from brookite to anatase. With increasing calcination temperature, the crystalline particle size and the anatase content increase. The lattice parameters of the pure TiO_2 structure are $a = b =$ 3.7812 Å and $c =$ 9.4854 Å. Compared to pure TiO_2, the changes of the a and c lattice parameters of TCS3, TCS4, and TCS5 were determined to be −0.0008, −0.0003, and −0.0002 Å, respectively, for a and 0.0253, 0.0192, and 0.0174 Å, respectively, for c. These results show that the lattice parameters remain almost unchanged along the a and b axes, whereas the c-axis parameters increase because of the presence of adventitious C and S. The c value increases relative to that of pure TiO_2 possibly because of both carbon interstitially doping and the larger ionic radius of S^{2-} (1.7 Å) compared to that of O^{2-}(1.22 Å).[13]

Table 1. Crystalline Particle Sizes, Crystal Phase Contents, and Lattice Parameters of Various Photocatalysts

samples	calcination temp (°C)	cryst particle size (nm)	cryst phase content (%)[a]	lattice parameters (Å)
pure TiO_2	550	15.8	A, 92.1; B, 7.9	$a = b = 3.7812$, $c = 9.4854$
TCS1	500	10.1	A, 79.4; B, 20.4	−
TCS2	550	14.6	A, 89.9; B, 10.1	−
TCS3	600	22.1	A, 100.0; B, 0	$a = b = 3.7804$, $c = 9.5107$
TCS4	600	25.5	A, 100.0; B, 0	$a = b = 3.7809$, $c = 9.5046$
TCS5	600	27.3	A, 91.7; R, 8.3	$a = b = 3.7810$, $c = 9.5028$

[a] A, anatase; B, brookite; R, rutile phase.

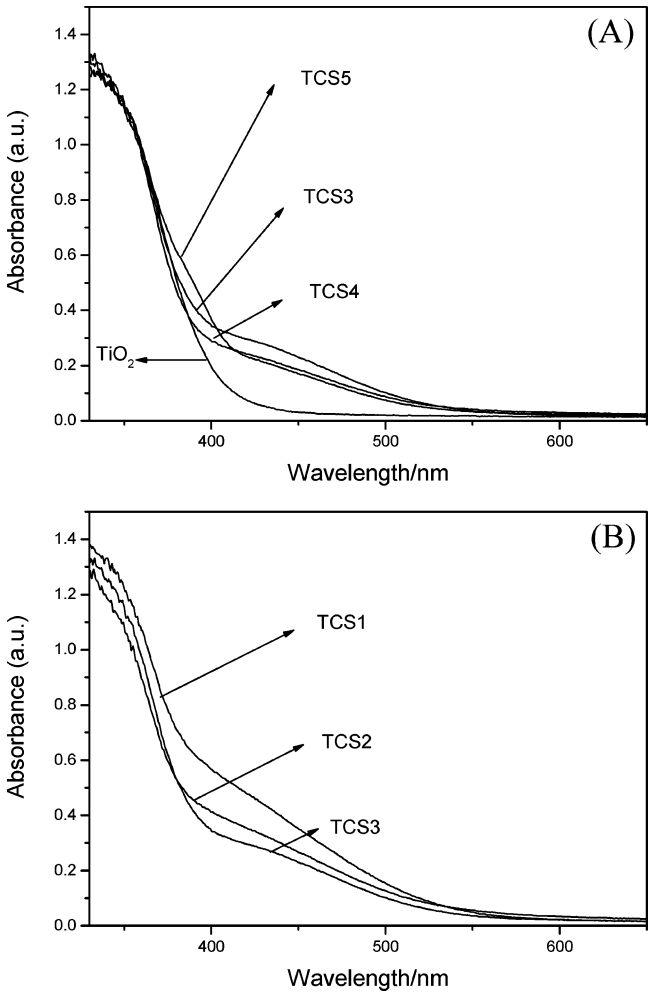

Figure 4. UV−vis diffuse reflectance absorption spectra of various photocatalysts: (A) effect of preparation method, (B) effect of calcination temperature.

3.4. UV−Vis Reflectance Spectroscopy. The samples prepared by different methods have different optical properties, as shown in Figure 4A. Pure TiO_2 has no ability to respond to visible light, whereas the absorption edges of the photocatalysts

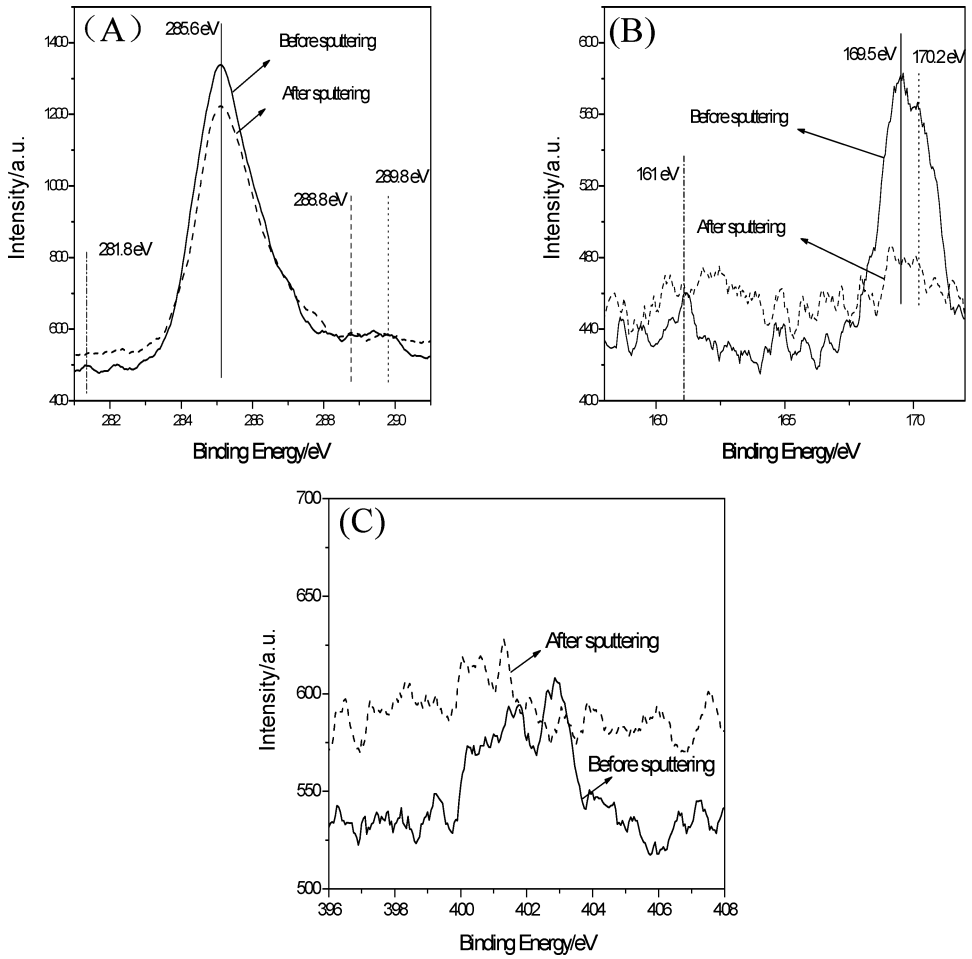

Figure 5. (A) C_{1s}, S_{2p}, and N_{1s} XPS spectra of TCS3 before and after sputtering.

codoped with carbon and sulfur are shifted into the visible region. The absorption intensities of the samples in the visible region are in the order TCS3 > TCS4 > TCS5. By evaluating the thresholds of the new absorptions of TCS3, TCS4, and TCS5 in the visible range, their band gaps were determined to be 3.02, 3.06, and 3.07 eV, respectively.

In our experiments, we observed that the yellow color of the photocatalysts prepared became much paler when the calcination temperature was increased from 500 to 600°C. The optical properties of some samples calcined at different temperatures are reported in Figure 4B. The absorption intensities of the samples in the visible region are in the order TCS1 > TCS2 > TCS3. For comparison, the band gap of as-prepared TiO_2 was determined to be 3.08 eV, and that of Degussa P25 is 3.10 eV (not shown here). The band gaps of TCS1, TCS2, and TCS3 were calculated to be 2.98, 3.01, and 3.02 eV, respectively. The absorption intensities and band gaps both decrease with increasing calcination temperature.

Both the difference in the optical properties and the change in the structures show that the effect of the wet chemistry process on catalysts is more apparent than that of the solid-state reaction. Furthermore, in comparison to pure TiO_2, the changes in the optical properties and structure of TCS5 seem less than those of TCS3 and TCS4, which were prepared from amorphous TiO_2. This suggests that the transition process from an amorphous state to anatase is important for the ion-doping process.

3.5. XPS Studies. To investigate the states of the doping ions, we applied XPS to record the C_{1s} and S_{2p} XPS spectra of TCS3 before and after Ar^+ sputtering, as shown in Figure 5. In Figure 5A, before sputtering, peaks at 281.8, 282.6, 285.6, 288.8, and 289.8 eV were found. The strongest signal, at 285.6 eV, arises from elemental carbon;[8] the peaks at 281.8 and 282.6 eV are due to Ti−C bonds;[11] and the other two peaks at 288.8 and 289.8 eV indicate the formation of carbonate species.[8] After sputtering, the peak at 285.6 eV remains strong. The peaks at 288.8 and 289.8 eV show that carbonate species still exist in the bulk. The peaks at 281.8 and 282.6 eV disappear, indicating the absence of Ti−C in bulk. The S_{2p} XPS spectra of TCS3 before and after sputtering are shown in Figure 5B. Before sputtering, two peaks at 169.5 and 170.2 eV are observed. The first peak is assigned to S^{4+} ions,[18] which reveals that 4+ sulfur ions replace 4+ titanium ions in the lattice, and the second is attributed to S^{6+}.[12,13] These ions are derived from sulfur dioxide molecules absorbed on the TiO_2 surface.[13] In addition, there is a weaker signal around 161 eV corresponding to the Ti−S bond, which is caused by the substitution of O^{2-} by S^{2-} in the TiO_2 lattice.[13] The finding that the two peaks decrease dramatically after sputtering reveals the presence of trace amounts of sulfur in the bulk.

The atomic composition of the sample of TCS3 before and after sputtering changes from 22.07% Ti, 58.03% O, 17.21% C, 1.48% S, and 1.21% N to 27.61% Ti, 58.7% O, 12.88% C, 0.81% S, and 0% N. Figure 5C shows the change in the N impurity. Before sputtering, some signals appear in the region of about 400−404 eV, which are assigned to hyponitrite.[4] However, after sputtering, most of the N signals disappear. This clearly indicates that the N impurity is just located in the surface region of sample and absent in the bulk.

3.6. Photodegradation of 4-Chlorophenol. 4-Chlorophenol is a ubiquitous pollutant that has no absorption in the visible

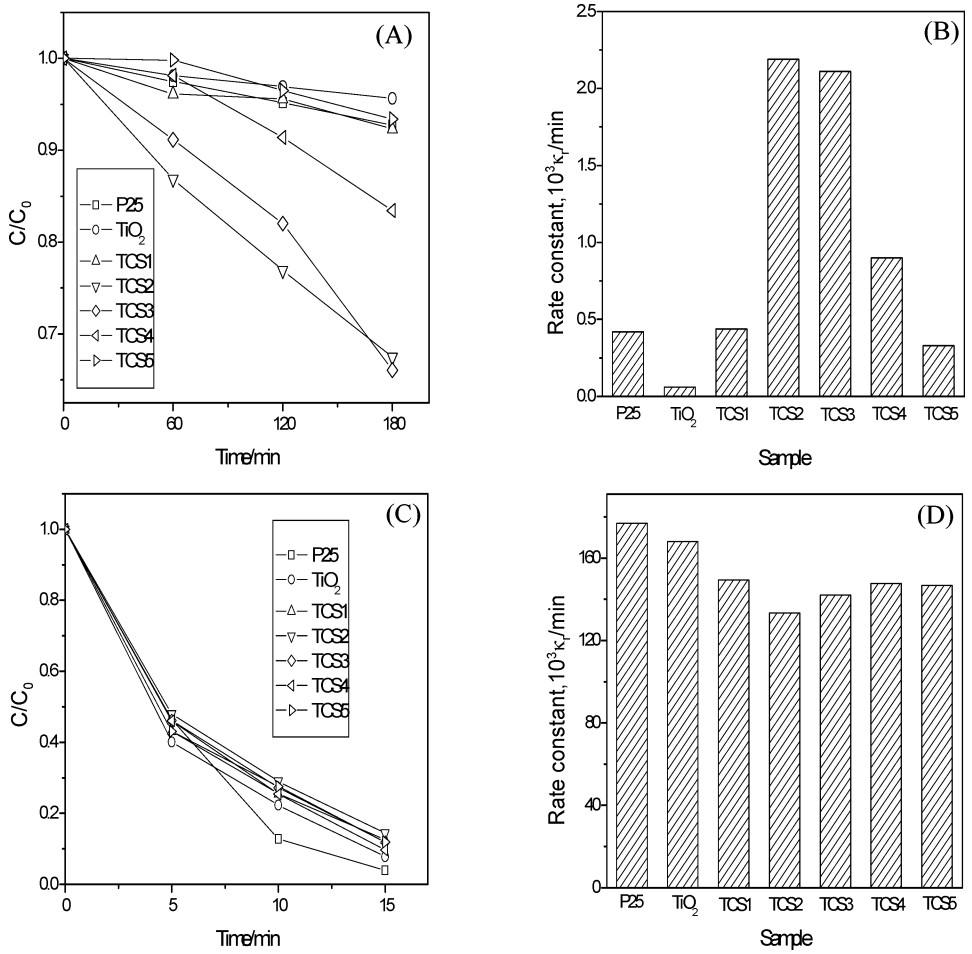

Figure 6. Degradation efficiencies and apparent rate constants for various samples under (A,B) visible and (C,D) UV irradiation.

region. Therefore, we selected it as a target contaminant chemical. The general photocatalytic reaction of 4-CP is

$$2C_6H_5OC1 + 13O_2 \xrightarrow{TiO_2,\ h\nu,\ H_2O} 12CO_2 + 4H_2O + 2HC1 \quad (1)$$

Generally, the photodegradation reaction of 4-CP can be described by the Langmuir−Hinshelwood mechanism. The photocatalytic activities of the as-prepared photocatalysts were studied by evaluating the apparent reaction rate constant k_a.[1,9,14] The photocatalytic degradation efficiencies and apparent rate constants of the various samples are displayed in Figure 6. For comparison, as-prepared pure TiO_2 and Degussa P25 were selected as reference samples, as shown in Figure 6. They are of low efficiency in the photodegradation of 4-CP under visible irradiation, and TCS2 exhibits the highest activity. The differences in efficiency among TCS1, TCS2, and TCS3 reveal the effects of calcination temperature. As shown previously, the calcination temperature affects the crystal phase, crystalline particle size, and optical properties of as-prepared codoped TiO_2. With increasing calcination temperature, these properties vary in close relation to the photodegradation efficiency under visible light. For example, a higher calcination temperature will result in a higher anatase phase content, which might be helpful for the photodegradation. Yet, a higher temperature will also increase the particle size, which might lead to a lower efficiency. Moreover, a higher calcination temperature decreases the absorbance of the catalysts in the visible region, which might weaken photocatalysis under visible irradiation. Carbon−sulfur-codoped TiO_2 calcined at 550 °C exhibited the highest photodegradation efficiency, which was possibly due to synergistic effect of various properties. To compare the effect of preparation method on the photocatalytic efficiency, we evaluated the photodegradation efficiencies of the samples prepared by various methods calcined at the same temperature. As shown in Figure 6A,B, the photocatalytic efficiencies of these samples are in the order TCS3 > TCS4 > TCS5, indicating that the activity of TCS3, prepared using the wet chemistry process, was higher than the activities of other samples obtained by the solid-state reaction.

Therefore, the wet chemistry process plays an important role in determining the photocatalytic activity of nonmetal-ion-doped photocatalyst. In addition to generating Ti−S bonds, the wet chemistry process also helps ion donors disperse with TiO_2 at the molecule level. Such dispersion will increase the combustion temperature and make combustion occur during the crystallization process, as, in this process, most of the ion-doping process occurs.

Figure 6 also shows the photocatalytic efficiencies of various samples under UV irradiation. Degussa P25 catalyst exhibits the highest efficiency in the degradation of 4-CP under UV light. The samples with high efficiencies under visible irradiation had low efficiencies under UV irradiation in our work. This indicates that the doping sites can also serve as recombination sites and hinder the separation of the photogenerated electrons and holes. Thus, the impurities lead to low efficiencies for TCS series under UV light.

4. Conclusions

A novel C−S-codoped TiO_2 material was synthesized by hydrolysis of tetrabutyl titanate in a mixed aqueous solution containing thiourea and urea. UV−vis reflectance spectroscopy showed that the catalyst can respond to visible light. Experiments on the photodegradation of 4-CP also revealed the capacity for photocatalysis under visible irradiation. The wet chemistry process is appropriate for ion doping because it can both make organic substances mix with precursors at the molecule level and lead to the formation of Ti−S bonds. Moreover, the crystallization process from an amorphous state to the anatase phase is also important for the ion-doping process.

Acknowledgment

This work was sponsored by the National Basic Research Program of China (No. 2003CB615702), the Scientific Research Foundation for Returned Overseas China Scholars, the State Education Ministry (2004527), and the Key Laboratory of Material-Oriented Chemical Engineering of Jiangsu Province and Ministry of Education.

Literature Cited

(1) Hoffmann, M. R.; Martin, S. T.; Choi, W.; Bahnemann, D. W. Environmental applications of semiconductor photocatalysis. *Chem. Rev.* **1995**, *95*, 69−96.

(2) Sato, S. Photocatalytic activity of nitrogen oxide (NO_x)-doped titanium dioxide in the visible region. *Chem. Phys. Lett.* **1986**, *123*, 126−128.

(3) Asahi, R.; Morikawa, T.; Ohwaki, T.; Aoki, K.; Tage, Y. Visible-light photocatalysis in nitrogen-doped titanium oxides. *Science* **2001**, *293*, 269−271.

(4) Sakthivel, S.; Janczarek, M.; Kisch, H. Visible light activity and photoelectrochemical properties of nitrogen-doped TiO_2. *J. Phys. Chem. B* **2004**, *108*, 19384−19387.

(5) Kobayakawa, K.; Murakami, Y.; Sato, Y. Visible-light active N-doped TiO_2 prepared by heating of titanium hydroxide and urea. *J. Photochem. Photobiol. A: Chem.* **2005**, *170*, 177−179.

(6) Ihara, T.; Miyoshi, M.; Iriyama, Y.; Matsumoto, O.; Sugihara, S. Visible-light-active titanium oxide photocatalyst realized by an oxygen-deficient structure and by nitrogen doping. *Appl. Catal. B: Environ.* **2003**, *42*, 403−409.

(7) Yin, S.; Yamaki, H.; Komatsu, M.; Zhang, Q. W.; Wang, J. S.; Tang, Q.; Saito, F.; Sato, T. Preparation of nitrogen-doped titania with high visible light induced photocatalytic activity by mechanochemical reaction of titania and hexamethylenetetramine. *J. Mater. Chem.* **2003**, *13*, 2996−3001.

(8) Sakthivel, S.; Kisch, H. Daylight Photocatalysis by Carbon-Modified Titanium Dioxide. *Angew. Chem., Int. Ed.* **2003**, *42*, 4908−4911.

(9) Lettmann, C.; Hildenbrand, K.; Kisch, H.; Macyk, W.; Maier, W. F. Visible light photodegradation of 4-chlorophenol with coke-containing titanium dioxide photocatalyst. *Appl. Catal. B: Environ.* **2001**, *32*, 215−227.

(10) Ohno, T.; Tsubota, T.; Nishijima, K.; Miyamoto, Z. Degradation of methylene blue on carbonate species-doped TiO_2 photocatalysts under visible light. *Chem. Lett.* **2004**, *33*, 750−751.

(11) Irie, H.; Watanabe; Y.; Hashimoto, K. Carbon-doped anatase TiO_2 powders as a visible-light sensitive photocatalyst. *Chem. Lett.* **2003**, *32*, 772−773.

(12) Ohno, T.; Mitsui, T.; Matsumura, M. Photocatalytic activity of S-doped TiO_2 photocatalyst under visible light. *Chem. Lett.* **2003**, *32*, 364−365.

(13) Yu, J. C.; Ho, W.; Yu, J. G.; Yip, H.; Wong, P. K.; Zhao, J. C. Efficient visible-light-induced photocatalytic disinfection on sulfur-doped nanocrystalline titania. *Environ. Sci. Technol.* **2005**, *39*, 1175−1179.

(14) Yu, J. C.; Yu, J. G.; Ho, W.; Jiang, Z. T.; Zhao, L. Z. Effects of F doping on the photocatalytic activity microstructures of nanocrystalline TiO_2 power. *Chem. Mater.* **2002**, *14*, 3808−3816.

(15) Hong, X. T.; Wang, Z. P.; Cai, W. M.; Lu, F.; Zhang, J.; Yang, Y. Z.; Ma, N.; Liu, Y. J. Visible-light-activated nanoparticle photocatalyst of iodine-doped titanium dioxide. *Chem. Mater.* **2005**, *17*, 1548−1552.

(16) Lin, L.; Lin, W.; Zhu, Y. X.; Zhao, B. Y.; Xie, Y. C. Phosphor-doped titania—A novel photocatalyst active in visible light. *Chem. Lett.* **2005**, *34*, 284−285.

(17) Bacsa, R.; Kiwi, J.; Ohno, T.; Albers, P.; Nadtochenko, V. Preparation, testing and characterization of doped TiO_2 active in the peroxidation of biomolecules under visible light. *J. Phys. Chem. B* **2005**, *109*, 5994−6003.

(18) Ohno, T.; Tsubota, T.; Nakamura, Y.; Sayama, K. Preparation of S, C cation-codoped $SrTiO_3$ and its photocatalytic activity under visible light. *Appl. Catal. A: Gen.* **2005**, *288*, 74−79.

(19) Hernan, L.; Morales, J.; Santos, J.; Eapinos, J. P.; Gonzalez-Elipe, A. R. Preparation and characterization of diamine intercalation compounds of misfit layer sulfides. *J. Mater. Chem.* **1998**, *8*, 2281−2286.

(20) Kwauk, M. S.; Li, J. H. Scale and structure in chemical engineering. *Trans. Inst. Chem. E A* **2002**, *80*, 699−700.

(21) Wei, J. Multiscale structure of uniformity in mixtures. *Ind. Eng. Chem. Res.* **1999**, *38*, 576−589.

Received for review March 22, 2006
Revised manuscript received May 11, 2006
Accepted May 13, 2006

IE060350F